

Physics Characterization of a Heterogeneous Sodium Fast Reactor Transmutation System

Global 2007

Samuel E. Bays

September 2007

The INL is a
U.S. Department of Energy
National Laboratory
operated by
Battelle Energy Alliance



This is a preprint of a paper intended for publication in a journal or proceedings. Since changes may be made before publication, this preprint should not be cited or reproduced without permission of the author. This document was prepared as an account of work sponsored by an agency of the United States Government. Neither the United States Government nor any agency thereof, or any of their employees, makes any warranty, expressed or implied, or assumes any legal liability or responsibility for any third party's use, or the results of such use, of any information, apparatus, product or process disclosed in this report, or represents that its use by such third party would not infringe privately owned rights. The views expressed in this paper are not necessarily those of the United States Government or the sponsoring agency.

Physics Characterization of a Heterogeneous Sodium Fast Reactor Transmutation System

Samuel E. Bays

Idaho National Laboratory
P.O. Box 1625, MS 3117, Idaho Falls, ID 83403
Samuel.Bays@inl.gov

The threshold-fission (fertile) nature of Am-241 is used to destroy this minor actinide by capitalizing upon neutron capture instead of fission within a sodium fast reactor. This neutron-capture and its subsequent decay chain leads to the breeding of even mass number plutonium isotopes. A slightly moderated target design is proposed for breeding plutonium in an axial blanket located above the active “fast reactor” driver fuel region. A parametric study on the core height and fuel pin diameter-to-pitch ratio is used to explore the reactor and fuel cycle aspects of this design. This study resulted in both a non-flattened and a pancake core geometry. Both of these designs demonstrated a high capacity for removing americium from the fuel cycle. A reactivity coefficient analysis revealed that this heterogeneous design will have comparable safety aspects to a homogeneous reactor of the same size.

I. INTRODUCTION

Generally, for low conversion ratio sodium fast reactors (SFR) with high minor actinide loaded fuels, there is a tradeoff between the optimal Doppler and void coefficients and the attainable minor actinide destruction efficiency. The two most basic SFR feedback mechanisms are the Doppler feedback provided by fertile uranium in the fuel and blankets; and the increase in axial neutron streaming that occurs during coolant voiding. A low conversion ratio can be attained by decreasing the parasitic capture while increasing leakage.¹

The tradeoff stems from the fact that the mechanisms commonly used to remove neutrons from the reactor during transients also remove them in steady state operation². For example, enhancing axial streaming with a pancake geometry or a reduced fuel pin diameter makes the void coefficient more negative. But, the increased overall leakage reduces the available excess reactivity. Alternatively, increasing fertile U-238 increases resonance capture and makes the Doppler coefficient more negative. However, this produces further transuranics from captures in the same resonances that provide the beneficial feedback. In both cases, more fissile plutonium is required to compensate for reactivity

lost by the modifying strategy. The added plutonium and lack of fertile material increases the reactor cycle reactivity swing.

The principle purpose for a low conversion ratio is the destruction of plutonium and possibly other undesired transuranics in the fuel cycle. For the current United States fuel cycle, the minor actinides: Np-237 and Am-241 are the space limiting isotopes to repository storage. This is because these isotopes have an even neutron number which gives them long half lives. It is also due to an even number of neutrons that make these isotopes have a threshold fission barrier of 1 MeV. Therefore, these SNF minor actinides are very difficult to be destroyed by fission because almost the entire flux in a SFR falls below this 1 MeV threshold. However, neutron capture in these “fertile” minor actinides leads to the generation of the even plutonium isotopes: Pu-238 and Pu-242. Though these plutonium isotopes still have an even neutron number, they are more *fissionable* than the starting minor actinides in the fast neutron spectrum. These even plutonium isotopes have very little fissile value in thermal reactors but have a significantly larger worth in fast reactors. Therefore, to increase the minor actinide destruction rate without the negative attributes of a low conversion ratio, it is desirable to first transmute them into plutonium via neutron capture.

Transmuted even isotope plutonium breeding can be accomplished with a thermalizing flux trap within the SFR. The goal of such a trap is to recover the fast neutrons leaked from the SFR and moderate them to a softer spectrum before irradiating a minor actinide rich target. Because enhanced axial leakage can be achieved with a flattened geometry, the targets are located in an axial blanket residing above a pancake active driver core. Because this core design is both spatially and spectrally heterogeneous, it is dubbed as a Heterogeneous Transmutation Sodium Fast Reactor (HT-SFR).

I.A. Description of Work

For this work, a parametric study is conducted on the effects of core flattening and heavy metal fuel content upon the transmutation performance of the axial targets.

Also evaluated is the: cycle length, excess reactivity, and “total core” Doppler coefficient and sodium void worth as a function of this parameter set. All these factors are related to axial leakage and parasitic capture. However, the plutonium generation in the axial targets creates an additional feedback within the fuel cycle that is also a function of reactor and fuel geometry. Therefore, the purpose of the parametric study is to evaluate the tradeoff between core performance factors and the maximum minor actinide destruction rate.

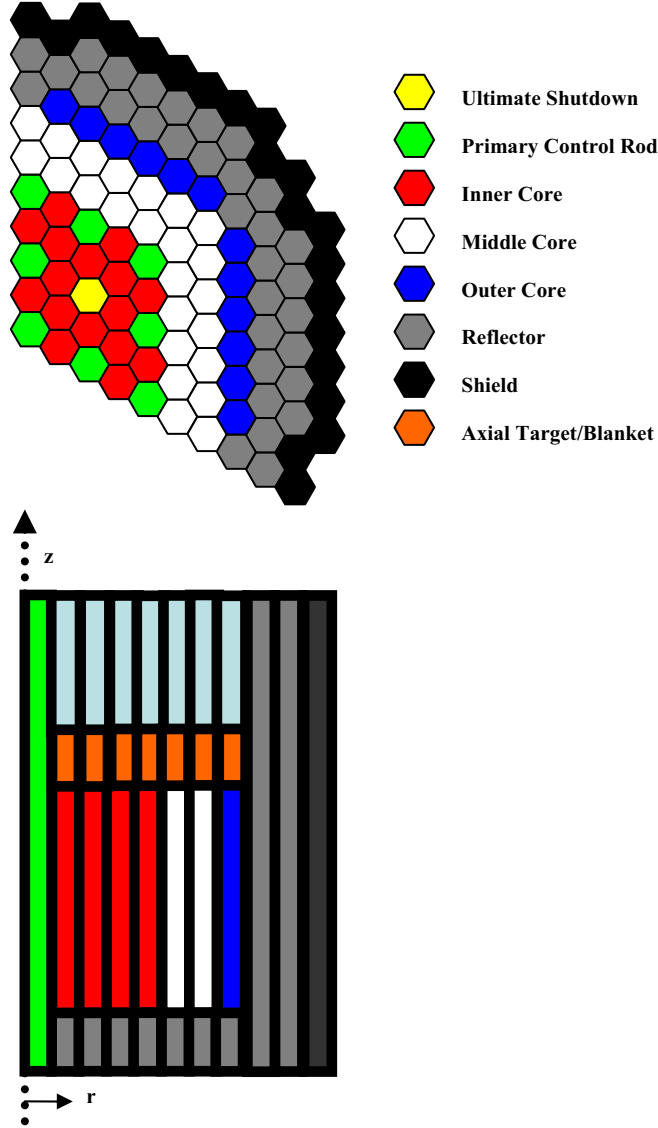


Figure 1: HT-SFR radial and r-z profiles (not an exact scale).

The target’s height and composition are held constant for all points in the parametric evaluation. They comprise a 20 cm tall axial blanket placed between the plenum and driver core of the 1000 MWth Advanced Burner Reactor (ABR) design proposed by Hoffman et al³. The lateral

core layout is assumed to be identical to the ABR case with a conversion ratio (CR) of 0.5 as shown in Figure 1. Starting with the ABR reference height of 101.6 cm, the active driver core height was varied to 51.6 cm in 10 cm increments. For each one of these active core heights, the range of pin diameter-to-pitch ratios shown in Table 1 was evaluated. The core average volumetric power density was held constant for each height reduction. This was done to give a representative cycle length for each height.

Next, the ABR (CR=0.5) reference was evaluated for each increment in pin diameter-to-pitch ratio. This homogeneous reference provides the constraining reactor performance parameters for down-selecting to a practical core height and pin diameter.

Table 1: Reference fuel assembly design for varying height-to-diameter ratio.

	p/d=1.1	p/d=1.176	p/d=1.293	p/d=1.357
fuel assembly pitch: cm	16.142	16.142	16.142	16.142
pins per assembly	271	271	324	540
Fuel Assembly Volume Fraction				
Fuel	34.27%	29.30%	22.08%	17.40%
Bond	11.42%	9.77%	7.36%	5.81%
Structure	25.73%	25.68%	26.41%	29.15%
Coolant	28.79%	35.25%	44.15%	47.60%

Finally, a core height and pin diameter is found that gives the highest transmutation efficiency while at the same time ensuring reactivity coefficients within the boundaries of the homogeneous reference. Using this core height and pin diameter combination, additional driver assemblies were added to the core until the HT-SFR thermal power output matched that of the 1000 MWth ABR to make the HT-SFR of commercial scale. This new core design demonstrates similar fuel cycle and reactor performance attributes as the core with the smaller radius from the parametric study.

I.B. Reactor Design and Fuel Cycle

Target fuel rodlets are placed adjacent to $\text{ZrH}_{1.6}$ dilution rods in an axial blanket configuration above the driver fuel. A zirconium metallic fuel alloy is assumed for both driver and target rods. Zirconium hydride was selected for its high thermal conductivity and melting temperature. The 1.6 H/Zr stoichiometric ratio was selected to get the zirconium hydride delta phase which does not change until 1000°C (REF.4). These rods are collocated within the same fuel pin and share the same plenum space with the driver fuel below them. The ratio of target to $\text{ZrH}_{1.6}$ containing fuel pins is five to one. Therefore, for a typical hexagonal SFR fuel assembly,

226 of the 271 fuel pins contain targets and 45 contain $\text{ZrH}_{1.6}$ above the driver fuel.

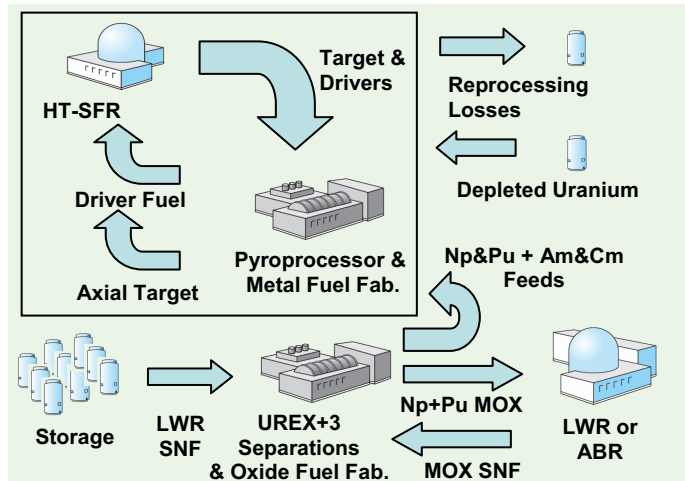


Figure 2: HT-SFR enabled fuel cycle service. The boxed off portion is the closed fuel cycle analyzed using the $\text{MC}^2\text{-2}$, DIF3D and REBUS.

The accompanying fuel management strategy allows the targets and driver fuel to be chopped and co-pyroprocessed together and refabricated into fresh driver fuel. Fresh targets are fabricated from the americium and curium component of SNF. This americium and curium stream is provided by the UREX+3 separations process. The UREX+3 neptunium and plutonium stream provides the external fissile feed to the driver fuel and a small amount in the targets. As seen in Figure 2, the SNF americium and curium is irradiated only once in targets before it rejoins the neptunium and plutonium in the driver. Therefore, sufficient americium must be destroyed in the targets such that the unburned americium is less than 5 w/o of the heavy metal in the driver. This ensures that the heterogeneous reactor's physics and fuel performance is comparable with the equivalent homogeneous ABR design⁵.

Similar to the ABR, the active driver fuel has no radial blankets and uses three enrichment zones to flatten the radial power profile across the core^{1 6 7}. The driver fuel composition is a TRU/U/10Zr (by weight) alloy. The ratio of middle and outer core enrichments to that of the inner core is: 1.25 and 1.50 respectively. The target fuel composition is 10Np&Pu/10Am&Cm/40U/40Zr. Some of the UREX+3 separated Np&Pu stream is diverted to provide an initial source of fissile material in the targets. This was done to minimize the target power swing and peaking during irradiation as a result of plutonium breeding. The target composition was selected for its similarity to the "uranium-free" AFC-1B tests irradiated at Idaho National Laboratory⁸.

II. CALCULATION METHODS

The Argonne fast reactor codes $\text{MC}^2\text{-2}$, DIF3D and REBUS are used for the reactor physics and fuel cycle calculations⁹. The $\text{MC}^2\text{-2}$ code was used to generate a 33 group cross section set for each enrichment zone, the axial blanket zone and reflectors and shields. Starting with an ultra-fine group ENDF-V/B cross section library, $\text{MC}^2\text{-2}$ created a collapsed cross section set by performing a zero dimensional infinite dilution critical buckling search using the extended P_1 method¹⁰. This zero-dimensional approach does not account for spatial shielding effects between the various core regions but for fast reactor calculations is generally sufficient due to the long neutron mean free path. The fast flux is almost entirely in the unresolved resonance range, thus making unresolved energy shielding and the unresolved resonance treatment the dominating effects in the group collapsing. $\text{MC}^2\text{-2}$ also performs a resolved resonance broadening treatment at user defined material and fuel temperatures. These cross sections are then used in a criticality calculation performed by DIF3D.

The DIF3D diffusion code was used to solve the multi-group steady state neutron diffusion equation using a hexagonal-z nodal coordinate system¹¹. In the nodal discretization, each hexagonal node in the lateral direction represents a fuel assembly. Because the mean free path is on the dimensional level of the fuel assembly, the individual fuel rods are homogenized across this hexagon.

REBUS uses DIF3D to perform a criticality search for the uncontrolled excess reactivity at each time step in its fuel depletion algorithm. Once the criticality search is completed, the fluxes from DIF3D are used in an exponential matrix to carry out the burnup, transmutation and decay of the fuel isotopic vector within the time step. This algorithm assumes that regional fluxes do not change significantly over this time step.

REBUS also performs the in-core fuel management and out-of-core cooling, reprocessing and refabricating for each reactor cycle. For the HT-SFR, REBUS's equilibrium cycle search option was used to carry out the fuel management steps depicted inside the boxed off portion of Figure 2. These operations were carried out until the excess reactivity and equilibrium cycle length was found. A maximum fuel burnup of 18 a/o after 6 reactor cycles (seven cycles for the outer core) was used to constrain the search procedure for the equilibrium cycle length.

Since REBUS only deals with the closed portion of the fuel cycle, the externally supplied UREX+3 feed is made sufficient to subsidize the pyroprocessor with enough heavy metal to constitute the next batch of fresh fuel. The isotopic vector for the UREX+3 feed was set constant to represent SNF discharged from a pressurized water reactor after a 51 MWD/kg irradiation and cooled for five years.

Once this equilibrium was attained, the Beginning of Equilibrium Cycle (BOEC) total core void and Doppler coefficients were calculated. The total core void worth was attained by copying the BOEC number densities from each isotope in each axial and radial region from the REBUS output file into a new DIF3D (no depletion) input file. The number density for sodium for each region was reduced by the coolant volume fraction. This way fuel assemblies only contained the bond sodium in the fuel rod gap with the coolant sodium voided. The sodium fraction was also reduced for the corresponding MC²-2 calculation.

The Doppler coefficient was calculated in a similar procedure without the change in sodium number density. Instead a new MC²-2 calculation was performed with all cross sections broadened at a temperature 100 K greater than that for the REBUS calculation. Then a new DIF3D calculation was performed with the BOEC number densities unchanged from the REBUS output file.

III. TARGET TRANSMUTATION PHYSICS

The repository space benefit stems principally from the removal of americium from the fuel cycle. This is because the repository's waste emplacement drift spacing is limited by the maximum rock temperature at the midpoint between them. The drift temperature is principally a function of the decay heat produced by Am-241 in the SNF. Because of its long half life, radiotoxicity, high solubility and low sorption in Yucca Mountain tuffs, Np-237 is the principle environmental concern to the biosphere if water does come into contact with the SNF. Because, Np-237 is the alpha decay product of Am-241, americium destruction in targets also minimizes the Np-237 accumulation in the repository.

Am-241 and Np-237 have an even neutron number and thus the binding energy contribution of an absorbed neutron is not sufficient to overcome the critical energy required for fission. In fact, the addition of a neutron to an odd-neutron nucleus (fissile isotope) to form an even-neutron compound nucleus gives a binding energy change that is about 1 MeV greater than for changing an even-neutron nucleus into an odd-neutron compound nucleus. This explains the fission threshold at one MeV for the long lived minor actinides Np-237 and Am-241.

A neutron capture in Np-237 generates the fissile Np-238 nucleus. However, Np-238 beta decays into Pu-238 with a short 2.117 day half-life. A neutron capture in Am-241 produces the fissile Am-242,242^m isotope. The yield fraction to the ground state is 80% in the fast spectrum. This Am-242 ground state beta decays into Cm-242 with a branching ratio of 83%. The other 17% of Am-242 electron captures into Pu-242. Cm-242 decays into Pu-238 with a 163 day half-life.

The Am-241 fission cross section below one MeV is two orders of magnitude less than fission above one MeV.

However, this capture cross section is almost as high as the Pu-239 fission cross section below one MeV. Therefore, the HT-SFR target neutron spectrum is moderated slightly in order to reduce the energy of leaked neutrons to just below 1 MeV. This increases the relative neutron capture in americium relative to plutonium fission in the targets.

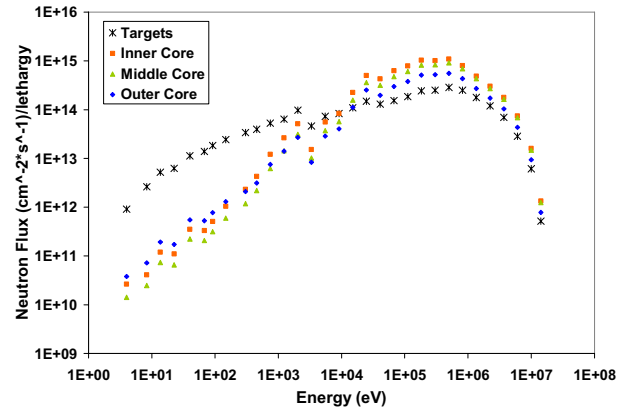


Figure 3: Target flux spectrum compared with the inner, middle and outer enrichment zone for a 101.6 cm tall HT-SFR with a pin-to-pitch diameter of 1.1.

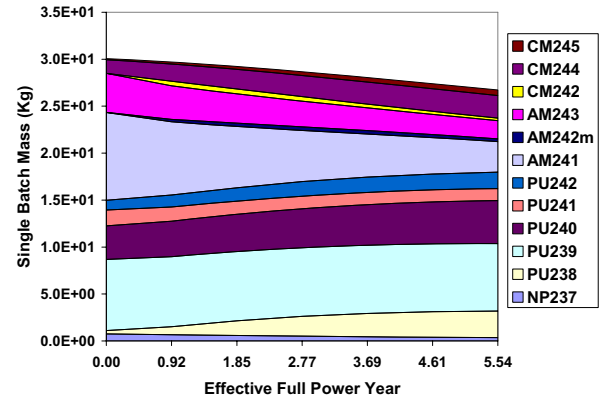


Figure 4: Change in isotope masses as a function of irradiation time for the target region residing above the middle core (core height = 101.6 cm, p/d=1.1).

The slight target moderation results in a relatively epithermal flux compared to that for the active driver regions as shown in Figure 3. It is important to note that though the total flux in the targets is less than in the active driver, much of it is being depressed by resonance absorption.

Much of the resonance absorption is in Pu-239 and U-238. However, resonance absorption in Pu-239 leading to fission serves to generate more neutrons. These neutrons have a relatively short mean free path that remains within the target's neutron population. Also, resonance absorption in U-238 serves to generate more

Pu-239. The combination of epithermal spectrum and plutonium breeding by both Am-241 and U-238 creates a plutonium breeding sub-critical blanket driven by neutrons leaked from the active core. As can be seen by Figure 4, the total amount of Pu-239 stays relatively constant. The total plutonium content increases mainly from Pu-238,242 production from Am-241 transmutation.

IV. PARAMETRIC STUDIES

Because the transmuted plutonium remains in the fuel cycle via the pyroprocessor, the amount of space reserved in the reactor for targets plays a significant role in the demand for the UREX+3 supplied Np&Pu. From a geometry standpoint, the ratio of target volume to core volume is dictated by the active core axial height. From a physics standpoint, the amount of Pu-239 breeding in the active core is a function of core flattening. Since, breeding excess Pu-239 in the active core is not a primary deliverable of the HT-SFR, it is desirable to minimize the active core's conversion ratio. Conversely, since breeding even plutonium is an indicator of americium destruction, it is desirable to maximize the target's conversion ratio.

IV.A. Moderator Effect

The rate of americium destruction is a function of the target spectrum, active core axial leakage and target rod volume. As will be discussed in a later section increasing the fuel rod diameter also increases the HT-SFR Am&Cm destruction rate. This is because increasing the target rod diameter also increases the amount of americium charged to the HT-SFR per cycle. If the reactor cycle is short, then the americium charge rate is increased. This does not, however, indicate the spectrum effect of the target hydrogen content. Because the target irradiation time is not held constant, simply comparing the ratio of charged to discharged target americium is not an adequate indication of the destruction efficiency. Instead, the fact that Am-241 is not easily produced from capture reactions in lesser mass isotopes is utilized to define a transmutation half-life. Therefore, Am-241 destruction can be characterized with a purely exponential behavior just as with radioactive decay. Table 2 shows the irradiation time required to reduce the americium mass by half.

Table 2: Transmutation Half-Lives (Years).

	p/d=1.1	1.176	1.293	1.357
101.6 cm	2.49	2.31	2.04	1.87
70.6 cm	2.73	2.54	2.24	2.06
50.6 cm	3.23	2.99	2.64	2.44

Notice, the shortest half-life is that for a full height active core with a very thin fuel pin. This can be explained by two effects. First, the smaller fuel pin indicates more active core leakage. Increased leakage requires higher plutonium enrichment for equivalent burnup. This higher plutonium content increases the active core fast flux and hence the flux leaked to the targets. This change in target flux for each pin design is plotted in Figure 5.

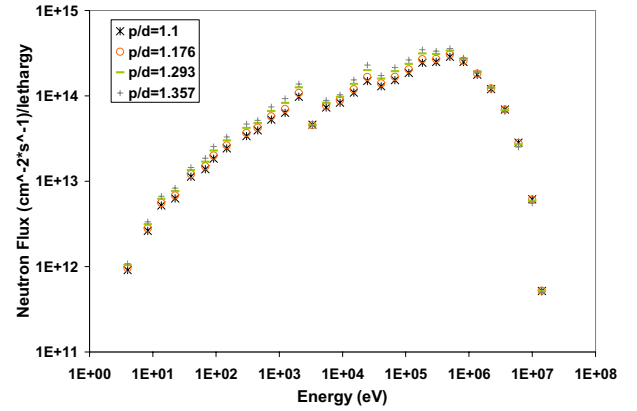


Figure 5: Target flux spectrum comparison for varying fuel pin-to-diameter ratio.

The decreasing half-lives with height are also related to axial leakage. Because of the enhanced leakage, the driver fuel radial power profile develops a depressed region in the inner core with increased flattening. The increase in the americium transmutation half-life with decreasing core height is caused by a reduction in the intensity of neutrons leaving the inner core region.

IV.B. Pancake Effect

It is important to note the conformity of the three power profiles plotted in Figure 6 in the outer core area. This behavior is indicative of the cosine shape of the radial flux gradient as neutrons leave the core. However, the axial power profile for the flattened core becomes less steep with decreasing axial height as shown in Figure 7. The combined effect of a depressed radial profile and the decreased total reactor power for decreasing height also decreases the overall target and driver burnup.

For the 51.6 cm tall core, the annular power profile is a result of poor optimization of the enrichment splitting for the flattened core design. Because neutron streaming is sufficient to flatten the inner core's power distribution, the enrichment splitting in the outer core regions may be reduced and the overall reactor power level increased. This un-optimized effect has the most significant impact on cycle length for cores with height less than 71.6 cm. The maximum burnup for this study is defined at the mid-plane of the inner most ring of driver fuel.

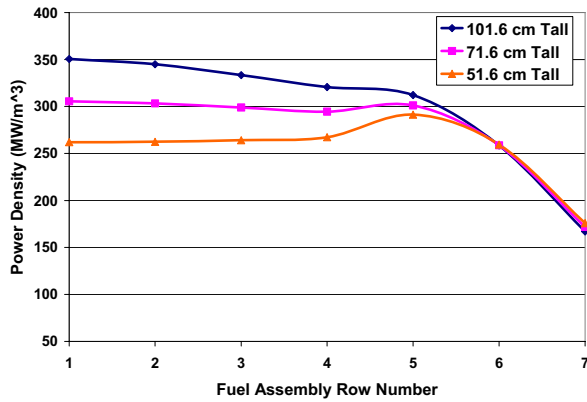


Figure 6: Active core radial power density profile for an HT-SFR with heights: 101.6, 71.6 and 51.6 cm ($p/d=1.1$).

Note: row five, six and seven have a higher enrichment than rows one through four.

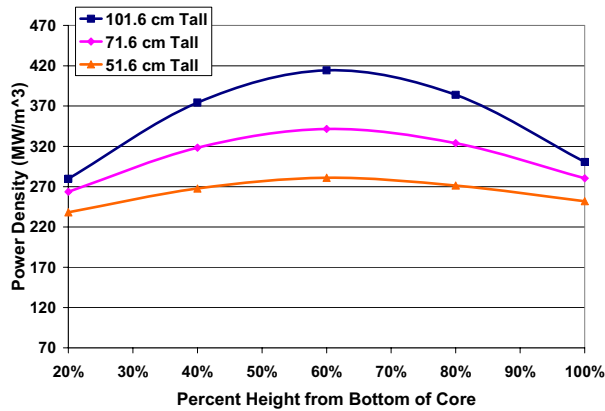


Figure 7: Inner core axial power density profile for an HT-SFR with heights: 101.6, 71.6 and 51.6 cm ($p/d=1.1$).

Therefore, the cycle length increase with core flattening, shown in Table 3, is being over predicted for heights less than 71.6 cm. The maximum burnup constraint in the outer core is being violated by a higher power density in the outer core. The next section describes two flattened core geometries at a 1000 MW power level with a corrected radial power distribution to compare the target transmutation performance.

Table 3: Cycle Length (EFPD).

	$p/d=1.357$	$p/d=1.293$	$p/d=1.176$	$p/d=1.1$
101.6 cm	2.01E+02	2.45E+02	3.02E+02	3.37E+02
91.6 cm	2.09E+02	2.55E+02	3.18E+02	3.55E+02
81.6 cm	2.19E+02	2.70E+02	3.37E+02	3.81E+02
71.6 cm	2.31E+02	2.85E+02	3.62E+02	4.08E+02
61.6 cm	2.44E+02	3.04E+02	3.91E+02	4.45E+02
51.6 cm	2.60E+02	3.27E+02	4.26E+02	4.90E+02

IV.C. Pin Diameter Effect

As mentioned earlier, increasing the fuel rod diameter also increases the volume of Am&Cm being charged to the axial targets. Flattening the driver while keeping the targets constant; increases the volume fraction that the axial blanket occupies within the HT-SFR. These factors increase the overall amount of plutonium transmuted in targets. Figure 8 shows the total rate of Am&Cm destruction for the entire HT-SFR.

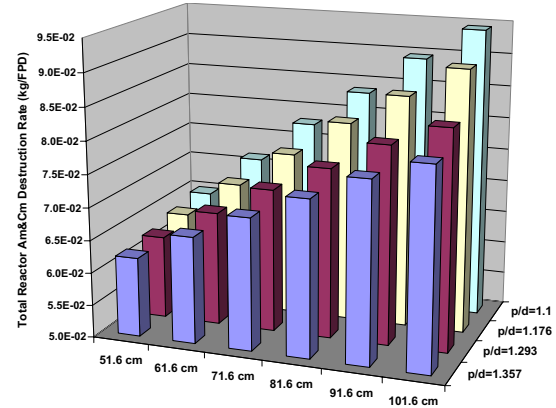


Figure 8: HT-SFR Am&Cm destruction rate as a function of core height and pin-to-pitch diameter.

This plot shows that the actual rate of Am&Cm destruction is not completely dictated by the transmutation half-life. It is more linked to the physical target volume. However, as was seen previously, the combined effect of reducing core height and reactor power also reduces the overall transmutation rate. This corresponds, partly, to the un-optimized radial power distribution for the flattened geometry.

Increasing the pin diameter also increases the amount of plutonium generation in the active core. This decreases the needed fuel enrichment to achieve the maximum fuel burnup. The inner core enrichment as a function of reactor height and fuel pin design is shown in Table 4. The enrichment reduction also reduces the BOEC excess reactivity as seen in Table 5. Because more plutonium is being bred in the active core from uranium, the cycle length also increases.

Table 4: Inner core enrichment.

	$p/d=1.357$	$p/d=1.293$	$p/d=1.176$	$p/d=1.1$
101.6 cm	35.42%	27.03%	18.84%	14.94%
91.6 cm	37.41%	28.60%	20.16%	16.17%
81.6 cm	39.87%	30.74%	21.85%	17.69%
71.6 cm	42.98%	33.28%	24.08%	19.66%
61.6 cm	47.12%	36.76%	26.83%	22.21%
51.6 cm	52.67%	41.37%	30.66%	25.67%

Reducing the BOEC excess reactivity reduces the required control rod worth. In turn, reducing the rod worth minimizes the reactors sensitivity to the control rod drive over-power accident initiation scenario.

Table 5: Excess Reactivity ($\rho_{\text{excess}} = \Delta k / k_{\text{avg}}$).

	p/d=1.357	p/d=1.293	p/d=1.176	p/d=1.1
101.6 cm	3.08%	2.77%	1.77%	0.88%
91.6 cm	3.23%	2.88%	2.04%	1.30%
81.6 cm	3.33%	3.18%	2.40%	1.69%
71.6 cm	3.43%	3.31%	2.87%	2.24%
61.6 cm	3.58%	3.62%	3.18%	2.79%
51.6 cm	3.62%	3.78%	3.65%	3.42%

V. DOWN-SELECTION

In order to validate the axial target design's efficacy, it is necessary to validate the HT-SFR against an equivalent homogeneous design. The ABR based homogeneous reference design is used to indicate the useful values from the previous parametric evaluation. The reactor performance comparison is made for equal fuel pin designs between the reference and HT-SFR. The range of applicable height is adjusted independently for each pin design so that the performance is only a function of flattening.

First, a one year cycle length is selected to synchronize HT-SFR refueling operations with a yearly cyclic commercial electric power demand. A range in capacity factor of 80% to 95% is assumed, which gives a cycle length range of 290 EFPD to 350 EFPD. Because of the un-optimized cycle length forecasts from above, this envelope is relaxed to 400 EFPD. This limits the fuel pin design in Table 3 to: $1.176 < h/d < 1.1$ and the core height to greater than 71.6 cm.

Next, the reference excess reactivity is used to establish the lower core height boundary for the $h/d=1.176$ and $h/d=1.1$ cases. This ensures a similar control rod worth (i.e.: boron concentration and/or B-10 enrichment) to that of the reference.

Table 6: Excess reactivity comparison with homogeneous reference case (Grey boxes indicate down-selection based on $\rho_{\text{exc}}^{\text{HT-SFR}} < \rho_{\text{exc}}^{\text{REF}}$).

	REF	HT-SFR			
	101.6 cm	101.6 cm	91.6 cm	81.6 cm	71.6 cm
p/d=1.1	1.31%	0.88%	1.30%	1.69%	2.24%
p/d=1.176	2.04%	1.77%	2.04%	2.40%	2.87%
p/d=1.293	3.02%	xx	xx	xx	xx
p/d=1.357	3.33%	xx	xx	xx	xx

As can be seen in Table 6, the maximum allowable excess reactivity is 2.04%. This allows a minimum height of 91.6.

Finally, the void and Doppler coefficients are used to narrow the core height selection. Minor actinides present in the driver fuel generally cause positive reactivity feedback from sodium voiding. This is because the loss of down scatters in sodium causes spectrum hardening with an increase in neutrons with energies greater than the fission threshold. The countering effect is the level of neutrons streaming out of the core. Therefore, the upper bound of the core height in Table 7 is reduced using the reference void coefficient as the constraint.

Table 7: Total void worth comparison with homogeneous reference (Grey boxes indicate down-selection based on $\rho_v^{\text{HT-SFR}} < \rho_v^{\text{REF}}$).

	REF	HT-SFR			
	101.6 cm	101.6 cm	91.6 cm	81.6 cm	71.6 cm
p/d=1.1	3.05%	3.18%	3.01%	xx	xx
p/d=1.176	3.31%	3.45%	3.26%	xx	xx
p/d=1.293	3.46%	xx	xx	xx	xx
p/d=1.357	3.25%	xx	xx	xx	xx

The HT-SFR active core is flattened to 91.6 cm in order to have a void worth less positive than the homogeneous reference case. This is expected because as discussed earlier, flattening the active core increases leakage. Lastly, the Doppler coefficient is used to pick between the two pin designs.

Table 8: Doppler coefficient comparison with the homogeneous reference case (Grey boxes indicate down-selection based on $\rho_{\text{dop}}^{\text{HT-SFR}} / \Delta T < \rho_{\text{dop}}^{\text{REF}} / \Delta T$).

	REF	HT-SFR			
	101.6 cm	101.6 cm	91.6 cm	81.6 cm	71.6 cm
p/d=1.1	-4.49E-06	xx	-5.05E-06	xx	xx
p/d=1.176	-4.17E-06	xx	-4.20E-06	xx	xx
p/d=1.293	-4.11E-06	xx	xx	xx	xx
p/d=1.357	-3.92E-06	xx	xx	xx	xx

The most fat fuel pin design is selected in Table 8 to give a Doppler coefficient that is more negative than the reference case. This is expected because the volume of fuel in the active core is increased and the percent of that fuel being uranium is increased. The increase in the uranium fraction is also the decrease in enrichment caused by increasing the pin diameter.

After down-selection, the final active core geometry is 91.6 cm with a 1.1 pin pitch-to-diameter ratio. Because, the core was only flattened by 10 cm, the radial power profile does not require additional optimization.

Hence, the burnup limit at the center/mid-plane and the expected cycle length is valid. In addition, the 355 day cycle length from Table 3 and the $8.95\text{E-}2$ kg/EFPD Am&Cm consumption rate from Figure 8 is valid.

VI. PANCAKE OPTION

Because of its closeness in physical volume is close to the homogenous reference, the down-selected HT-SFR's power level is increased to 1000 MWth. This core design represents a heterogeneous reactor with comparable reactor performance and safety attributes to the homogeneous reference. For comparison, a second core design with a 71.6 cm height is evaluated to observe a much larger target/driver ratio. An additional row of "outer core" drivers is added so that the power density and total power is made comparable to the "tall" HT-SFR (Figure 9). The enrichment splitting for this "pancake" HT-SFR is modified to give a flattened cosine radial power distribution. The pancake-core's middle and outer zones are enriched to 1.12 and 1.25 times that for the inner core respectively.

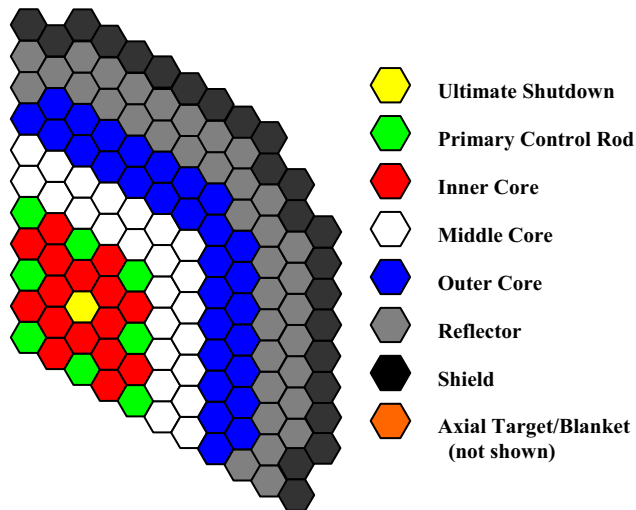


Figure 9: Pancake (eight rows of fuel) HT-SFR.

This enrichment splitting gives the pancake-core a much flatter power distribution than the tall-core. The axial leakage works in parallel with the enrichment splitting to create an almost completely flat power profile across the inner and middle enrichment zone. Figure 10 shows the radial power distribution for six axial slices through the core.

This initial estimation of the optimized enrichment splitting is sufficient enough to guarantee the highest power density in the inner core. Yet, it is apparent that the level of core flattening and the enrichment splitting could be varied independently until a true optimized power distribution is found.

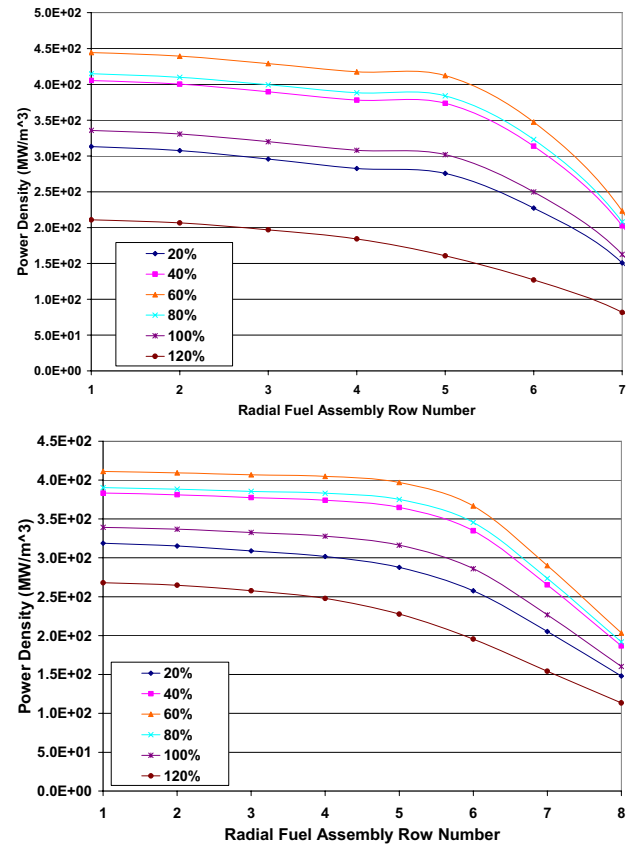


Figure 10: Radial power density profile for six axial slices through the core: Axial height is represented as a percentage of the full core height. (top = "tall", bottom = "pancake")

In either case, the radial power profile falls off sharply in the outer three rows of fuel. It is important to note, the volume ratio of these outer three rows to the rest of the core decreases with increasing core radius. Hence, the pancake-core's targets have a smaller contact area exposed to these low power rows.

Notice, the axial target power density is overall greater in the pancake-core than the tall-core. The increased target power density is linked to the axial leakage from the active core. As seen in the transmutation half-life discussion, flattening the core reduces the axial radial flux profile's curvature. This more shallow axial power profile provides a higher power density at the core axial periphery as seen in Figure 11. This increased power also provides for a reduced transmutation half-life of 2.22 years. Therefore, the Am&Cm destruction efficiency is actually more comparable to the thin fuel pin design. This higher efficiency combined with a larger overall target volume (more driver assemblies) gives a higher Am&Cm destruction rate compared with the "tall" core. This higher Am&Cm destruction rate equates into a higher

plutonium breeding rate. This increases the amount of Am&Cm and reduces the amount of Np&Pu drawn from the UREX+3 plant. Hence, the size of the surplus Np&Pu feed increases.

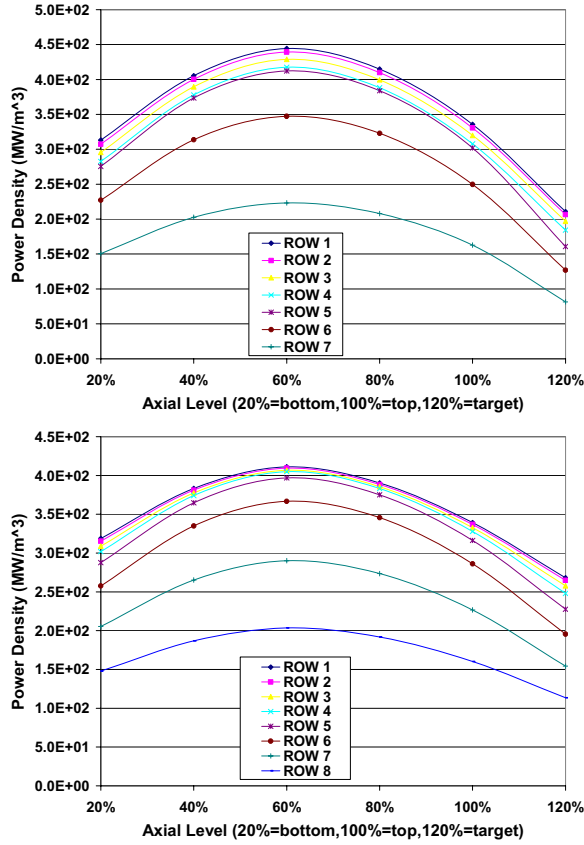


Figure 11: Axial power density profile for each row of fuel: Axial height is represented as a percentage of the full core height.
(top = “tall”, bottom= “pancake”)

In fact for both the “tall” and “pancake” designs, the external Np&Pu feed for the active core is reduced to zero for the equilibrium fuel cycle. Consequently, the UREX+3 plant only needs enough Np&Pu to produce fresh targets.

Table 9 shows the fuel cycle parameters for the homogeneous reference, “tall” and “pancake” cores. The “pancake” core has a greater amount of Am&Cm being destroyed in the targets. The “tall” HT-SFR has a shorter cycle length which gives it a higher Am&Cm feed rate. Though the “pancake” core has a more efficient target, it discharges a larger Am&Cm volume to the pyroprocessor. The “tall” core has a less efficient target but the shorter cycle length increases the rate that Am&Cm is charged to targets and thus received by the pyroprocessor. In both cases, the amount of Am&Cm diluted in the driver fuel is comparable to the reference and less than the 5% limit discussed earlier. This driver fuel Am&Cm is effectively

burned in the active core to the point where its quantity is stabilized in the HT-SFR fuel cycle.

Because both “tall” and “pancake” HT-SFR types are equally capable of destroying comparable amounts of Am&Cm, other non-physics related parameters must be considered to determine the preferred design from an economics and deployment standpoint. Chief among these is the added steel needed to increase the core barrel diameter for the pancake design. Equally important is the sizing of the gas plenum and its effect on the overall reactor height. Though the pancake core requires a slightly larger core barrel, it also makes available 30 cm of length within the fuel pin that can be used to increase the gas plenum height. A longer gas plenum is necessary to accommodate the helium gas production associated with the Cm-242 alpha decay in the Am-241 transmutation path to Pu-238.

Table 9: HT-SFR fuel cycle comparison.

	reference	tall	pancake
IC Enrichment	14.92%	16.07%	18.65%
Cycle Length (EFPD)	322.86	319.90	350.58
OC Am/HM ⁺	0.00%	1.72%	1.79%
OC MA/HM ⁺	1.06%	3.20%	3.40%
Am&Cm Target Dest Rate (kg/EFPY)	xx	1.48E+01	2.07E+01
Am&Cm Feed Rate (kg/EFPY)	2.79E+00	3.63E+01	3.31E+01
Np&Pu Feed Rate (kg/EFPY)	4.84E+01	3.60E+01	4.31E+01
HM Feed Rate (kg/EFPY)	3.75E+02	3.80E+02	3.75E+02
IC Target Am Half-Life (Yr)	xx	2.49	2.22
Excess Reactivity	1.31%	1.12%	1.70%

⁺ Because the outer core has the highest enrichment, it is used for the minor actinide to heavy metal comparison for fresh driver assemblies.

VII. CONCLUSIONS

Earlier studies indicate that a low conversion ratio SFR is necessary to destroy the undesired transuranics waste isotopes found in SNF. From a physics standpoint a low conversion ratio is ideal for reducing the production of plutonium and minor actinides by reducing parasitic capture. This work makes a fundamental change in philosophy regarding minor actinide waste management. Previous repository studies recognize the Am-241 concentration within transuranic waste as the most limiting isotope for the SNF amount that can be stored in a geologic repository. Because this isotope is not fissile, its removal from the fuel cycle is best achieved by

parasitic capture. Because parasitic capture in americium leads to a transmutation path ending in even mass number plutonium isotopes, it can be used as a fertile blanket material.

Parametric studies were performed on a SFR with slightly moderated americium targets in the axial blanket. This HT-SFR parametric analysis revealed that high americium destruction in axial targets is achievable by flattening the active driver core. Recovering neutrons in the targets allows the active core to have a high axial neutron leakage which enhances void performance. Because the fuel cycle goal is now to destroy americium and not plutonium, a low conversion ratio is not necessary. This reduces the high reactivity swing associated with low conversion ratio reactors. It also relaxes the core flattening and fuel pin diameter reduction needed to attain a low conversion ratio. However because of the americium content in the driver fuel, some height reduction is necessary to ensure a void coefficient comparable with an equivalent homogeneous design. This comparison was made for the “tall” (91.6 cm) version of the HT-SFR. The “tall” HT-SFR required only a 10 cm height reduction to have a void coefficient comparable with the homogeneous reference.

Reducing the core height decreases the curvature of the axial power profile by increasing the axial leakage. This axial leakage places more flux in the axial targets for decreasing core height. Increasing the transverse axial flux increases the capture reaction rate. This reduces the Am-241 transmutation half-life. The transmutation half-life is used as an indicator of the transmutation efficiency because it is a direct reflection of the flux and neutron spectrum in which the targets are exposed. It was also found that if the height is made sufficiently small, the radial power profile of the inner and middle core can be flattened by axial leakage. For the “pancake” HT-SFR, this effect resulted in a lesser degree of enrichment splitting.

This pancake case had a smaller transmutation half-life than the taller core. The pancake core’s target volume was increased by adding an eighth row of fuel assemblies. The combination of these effects allowed the pancake reactor to have a higher reprocessing feedback of target bred plutonium in the fresh charge of driver fuel. Though the taller core had less breeding in targets, the internal Pu-239 breeding in the driver fuel from U-238 compensated for this deficiency. In fact for both tall and pancake cores, pyroprocessing provided all of the plutonium used in the driver fuel.

Both the tall and pancake HT-SFR are equally capable at sequestering americium from the fuel cycle. Further scoping calculations are necessary to determine the relative impact of a longer plenum height for collecting transmutation helium. The pancake HT-SFR allows for more plenum space but also requires a larger core barrel which entails a higher construction cost. The

taller HT-SFR would not have a larger core barrel than the homogeneous core but does not have any additional plenum space for transmutation helium. Therefore, the fuel assembly height would have to be increased to have a taller plenum which would incur a higher pressure loss in the thermal-hydraulic design.

Future work will perform these scoping calculations to gain some economic insight of the core size effects. Also, planned is an economic evaluation for deploying the surplus Np&Pu in MOX for commercial light water reactors. Next, future work will focus on constraining the HT-SFR’s cycle length by the maximum fuel cladding atom displacement damage.

Finally, the decay contribution from Cm-244 and the neutron emission from Cf-252 at various stages in the fuel cycle will be addressed. Cf-252 is produced by successive neutron capture from Cm-244. Cm-244 is produced by neutron capture in Am-243 followed by beta decay ($T_{1/2}=10.1$ hr) from Am-244. As is shown in a separate topical paper of this proceeding, the SFR is very effective at *stabilizing* the mass of americium and curium accumulated in the closed fuel cycle¹². The Cm-244 and Cf-252 may be high in the axial targets when discharged. However, the actual average amount of Cm-244 and Cf-252 present in the fuel cycle may be similar to that of the homogeneous reference.

A high americium destruction rate has been demonstrated for a slightly moderated target design in the axial blanket of a flattened sodium fast reactor. A “total core worth” reactivity coefficient analysis revealed that this heterogeneous design will have comparable safety aspects to a homogeneous reactor of the same size.

ACKNOWLEDGEMENTS

This work was supported by Idaho National Laboratory as part of the author’s PhD dissertation project. The author would like to thank James Tulenko, Max Salvatores, Steve Herring and Mehdi Asgari for their mentoring of this work.

REFERENCES

¹ Morris, E., Smith, M. (2002) Development of Low Conversion Ratio Fast Reactors for Transmutation, Argonne National Laboratory, ANL-AAA-057

² Choi, H., Downar, T. (1999), A Liquid-Metal Reactor for Burning Actinides of Spent Light Water Reactor Fuel-I: Neutronics Design Study, Nuclear Science and Engineering, 133, 1-22, Sept. 1999

³ Hoffman, E., Yang, W., Hill, R. (2006) Preliminary Core Design Studies for the Advanced Burner Reactor

Over a Wide Range of Conversion Ratios, Argonne National Laboratory, ANL-AFCI-177

⁴ Moore, K., Young, W., (1968), Phase Studies of the Zr-H System at High Hydrogen Concentrations, *Journal of Nuclear Materials*, 27, 316-324, September 1968

⁵ Stanculescu, A., Garnier, J., Rouault, J., Kiefhaber, E., Sunderland, R., (1994), Plutonium Burning and Actinide Transmutation in Fast Reactors: First Results Obtained within the Frame of the CAPRA Programme, *International Nuclear Congress Atoms for Energy (ENC '94)*, 2, 558-565, Lyon, France, October 2-6, 1994

⁶ Wade, D., Hill, R., (1997), The Design Rationale of the IFR, *Progress in Nuclear Energy*, 31, 1-2, 13-42, 1997

⁷ Hill, R., Wade, D., Liaw, J., Fujita, E., (1995), Physics Studies of Weapons Plutonium Disposition in the Integral Fast Reactor Closed Fuel Cycle, *Nuclear Science and Engineering*, 121, 17-31, Sept. 1995

⁸ Hilton, B., Hayes, S., Chang, G., (2006), Irradiation Performance of Fertile-Free Metallic Alloys for Actinide Transmutation, *Proceedings of the 11th Workshop on the Research, Deployment and Implementation of Fissile-Free Nuclear Fuels*, Park City, UT, October 10-12, 2006

⁹ Toppel, B. (1983), A User's Guide to the REBUS-3 Fuel Cycle Analysis Capability, Argonne National Laboratory, ANL-83-2

¹⁰ Henryson, H., Toppel, B., Stenberg, C., (1976), MC²-2: A Code to Calculate Fast Neutron Spectra and Multigroup Cross Sections, ANL-8144

¹¹ Derstine, K., (1984), DIF3D: A Code to Solve One-, Two-, and Three-Dimensional Finite-Difference Diffusion Theory Problems, ANL-82-64

¹² Asgari, M., Bays, S., Ferrer, M., Forget, B., (2007), Minor Actinide Transmutation for Low Conversion Ratio Sodium Fast Reactors, *Proceedings of Global 2007 – Advanced Nuclear Fuel Cycles and Systems*, Boise, ID, September 9-13, 2007